View metadata, citation and similar papers at core.ac.uk

brought to you by CORE

provided by IntechOpen

We are IntechOpen, the world's leading publisher of Open Access books Built by scientists, for scientists

4,800
Open access books available

122,000
International authors and editors

135M
Downloads

Our authors are among the

154
Countries delivered to

TOP 1%
most cited scientists

12.2%
Contributors from top 500 universities

CLARIVATE ANALYTICS BOOK CITATION INDEX INDEXED

WEB OF SCIENCE™

Selection of our books indexed in the Book Citation Index in Web of Science™ Core Collection (BKCI)

Interested in publishing with us?
Contact book.department@intechopen.com

Numbers displayed above are based on latest data collected.
For more information visit www.intechopen.com

Chapter 9

Microscopic Investigations on Woody Biomass as Treated with Ionic Liquids

Toru Kanbayashi and Hisashi Miyafuji

Additional information is available at the end of the chapter

http://dx.doi.org/10.5772/62721

Abstract

Woody biomass is one of the most promising renewable alternatives to fossil resources. However, some physical and chemical treatment is required to convert their chemical components into biofuels and valuable chemicals because of their low degradative properties. Recently, there has been considerable interest in ionic liquid treatment for biorefinery, and many fundamental studies on the reactivity of wood with ionic liquids have been performed from a chemical and morphological point of view. This chapter highlights the findings regarding morphological and topochemical features of wood cell walls in the degradation process as a result of ionic liquid treatment. Bright-field microscopy and scanning electron microscopy have revealed the swelling behavior of cell walls and the detailed ultrastructural features of wood tissues treated with ionic liquid. Polarized light microscopy and confocal Raman microscopy have clarified the changes in cellulose crystallinity and distribution of chemical compositions such as polysaccharides and lignin during ionic liquid treatment at the cellular level.

Keywords: Biorefinery, Cell wall, Liquefaction, Ionic liquid, Wood

1. Introduction

The efficient use of lignocellulosics has been an important approach to prevent exhaustion of fossil resources and global warming caused by increasing emissions of greenhouse gases. Among the various types of lignocellulosics, woody biomass is regarded as a promising resource because it is carbon neutral, abundantly available in many regions, and does not compete with agricultural production. Wood cell walls decompose to form persistent organic complexes mainly composed of cellulose (40–50%), hemicellulose (25–35%), and lignin (18–35%) [1, 2]. To convert

INTECH
open science | open minds

© 2016 The Author(s). Licensee InTech. This chapter is distributed under the terms of the Creative Commons Attribution License (http://creativecommons.org/licenses/by/3.0), which permits unrestricted use, distribution, and reproduction in any medium, provided the original work is properly cited. CC BY

their chemical components into transportable biofuels and chemical feedstocks, it is necessary to develop the processing technology to break their rigid structure. To date, various conversion methods such as acid hydrolysis [3–5], enzymatic saccharification [6, 7], pyrolysis [8–10], and supercritical or sub-critical fluid treatment [11–13] have been investigated. However, practical methods have not yet been established.

Ionic liquids are defined as organic salts with low melting points, and have many advantages including negligible vapor pressures, chemical and thermal stability, non-flammability, low viscosity, and reusability [14–16]. In addition, they can dissolve a wide range of organic and inorganic substances [14]. Ionic liquid treatment is attractive as a new conversion technology for woody biomass. **Figure 1** shows the typical cations and anions found in ionic liquids. There are an infinite number of combinations of cations and anions, and their physical properties, such as melting point, viscosity and dissolving power, can be easily changed by altering the combination. This is why ionic liquids are called "designer solvents" [17].

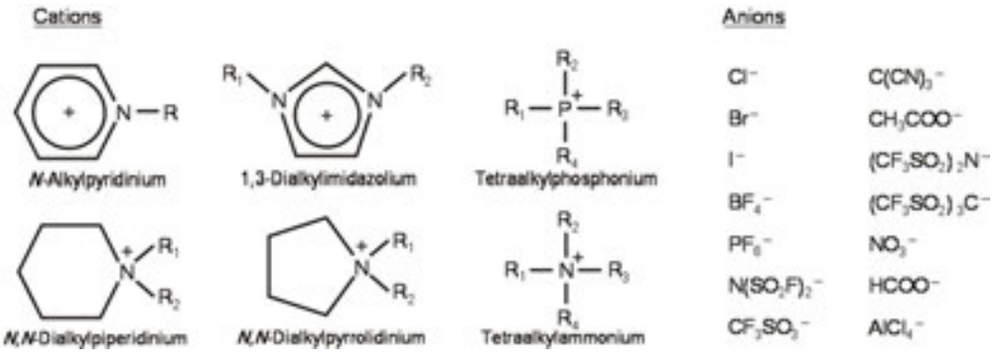

Figure 1. The structures of typical cations and anions in ionic liquids.

Recent studies revealed that certain types of ionic liquids can liquefy cellulose [18–20], lignin [21], and even wood cell walls [22–26]. Using ionic liquids as the solvent to process woody biomass, many fundamental studies on the reaction behavior of wood in ionic liquids have been carried out focusing on the chemical processes [27–31]. However, woody biomass is a very inhomogeneous composite at the cell level. Wood comprises various types of tissues such as the tracheid, wood fibers, vessels, and parenchyma. In addition, wood cell walls consist of several layers: a compound middle lamella (middle lamella + primary wall; CML) and a secondary wall (S), which is generally composed of S_1, S_2, and S_3 sublayers. The chemical components and distribution vary depending on the wood species, types of tissues and their layers [32]. Therefore, to improve the chemical conversion process using ionic liquids, a better understanding of the effects of ionic liquid treatment of wood, such as the interaction of wood with ionic liquids at the cell level and the deconstruction behavior of various types of tissues in ionic liquids, are required.

In this chapter, we focus on morphological and topochemical studies on the liquefaction of wood in ionic liquids, especially 1-ethyl-3-methylimidazolium chloride ([C2mim][Cl]) and 1-ethylpyridinium bromide ([EtPy][Br]), using various microscopy techniques. [C2mim][Cl] and [EtPy][Br] are known as the ionic liquids which can preferentially liquefy cellulose [25] and

http://dx.doi.org/10.5772/62721

lignin [31], respectively. Bright-field microscopy and polarized light microscopy were employed to determine the swelling and decomposition behaviors of wood cell walls and the state of cellulose crystallinity during ionic liquids treatment. Scanning electron microscopy (SEM) was used to observe the detailed ultrastructural changes in various wood tissues treated with ionic liquids. Confocal Raman microscopy was employed to examine the changes in chemical components including polysaccharides and lignin at the cellular level and to visualize their distribution on the cell walls during ionic liquids treatment.

2. Application of microscopy techniques to examine wood liquefaction

2.1. Light microscopy analysis

Morphological features of wood cell walls during the liquefaction process in ionic liquid were determined by light microscopy [33–38]. **Figure 2** shows bright-field microscopy and polarized light microscopy images of *Cryptomeria japonica*, which is the most common softwood species in Japan, treated with [C2mim][Cl] at 120°C for 0 h and 24 h. All the cell walls swelled after 24 h of [C2mim][Cl] treatment (**Figure 2c**). Although the cell walls of tracheids in latewood (summerwood; formed late in the growing season) were disordered and distorted after the treatment, those in earlywood (springwood; formed early in the growing season) were barely changed. The polarized light microscopy studies show that the brightness from the birefringence of cellulose in both earlywood and latewood was decreased after treatment (**Figure 2d**). These results imply that the crystalline structures of cellulose in wood are amorphized before the wood cell walls liquefy completely during [C2mim][Cl] treatment.

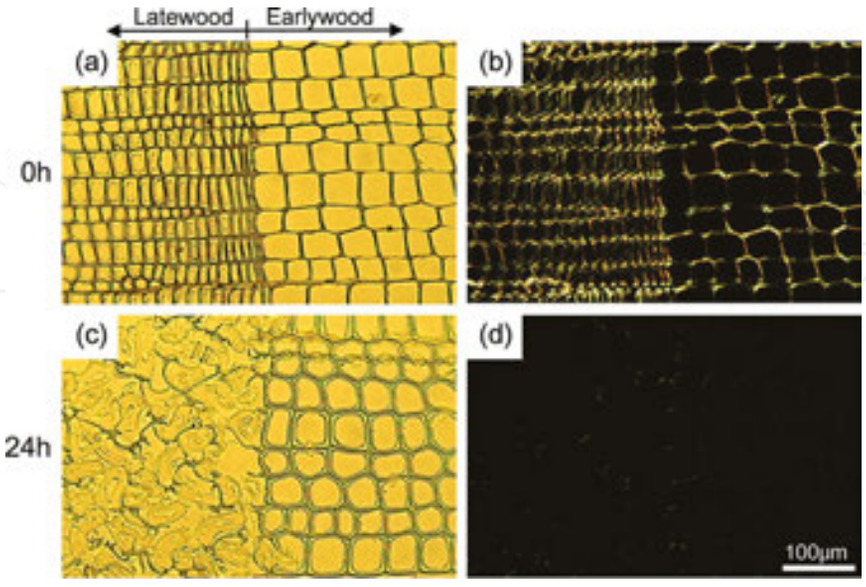

Figure 2. Bright-field microscopy (**a**, **c**) and polarized light microscopy images (**b**, **d**) of transverse sections of *Cryptomeria japonica* before (**a**, **b**) and after treatment with [C2mim][Cl] at 120°C for 24 h (**c**, **d**).

To study the detailed swelling behavior of tracheids arising from [C2mim][Cl] treatment, we performed time sequential measurements of the cell wall area, cell lumen area, and the total of cell lumen and cell wall areas, in earlywood and latewood, in transverse sections (**Figure 3**). The cell wall area in earlywood increased only slightly at an early stage of [C2mim][Cl] treatment, whereas that in latewood increased significantly. After the initial swelling, the cell wall area in earlywood showed no further changes, whereas that in latewood increased gradually with prolonged treatment time. After 72 h of treatment, the cell wall area in earlywood and latewood had increased by 1.5 and 4 times, respectively. These results indicate that the swelling behavior of the tracheids of *Cryptomeria japonica* is different for the two morphological regions. In particular, tracheids in latewood are more prone to swelling and being broken after [C2mim][Cl] treatment.

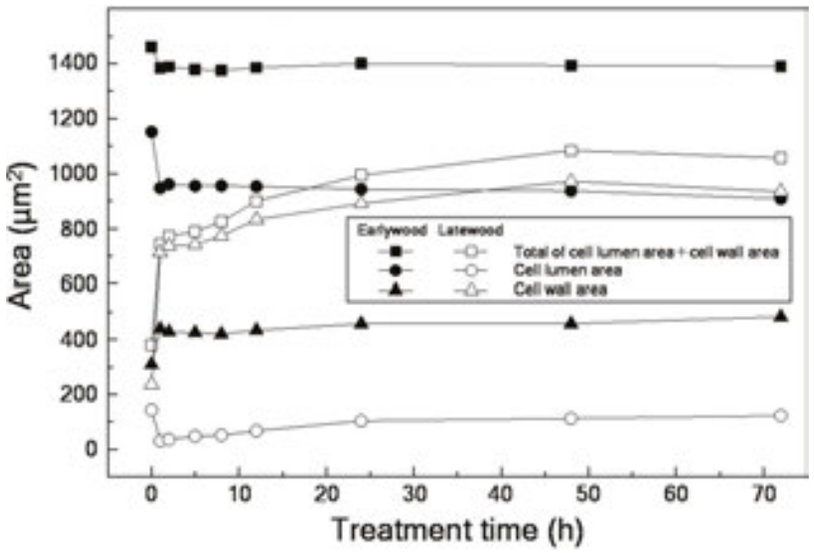

Figure 3. Changes in cell wall area, cell lumen area, and total of cell lumen + cell wall area in earlywood and latewood of *Cryptomeria japonica* during [C2mim][Cl] treatment at 120°C [34].

Changes in the cell wall area of fibrous cells of various Japanese hardwood species during [C2mim][Cl] treatment were also measured (**Figure 4**). At the initial stages of [C2mim][Cl] treatment, the cell wall areas of all species increased rapidly. Thereafter, the cell wall areas of *Fagus crenata* and *Quercus mongolica* in both earlywood and latewood increased continuously with progressing treatment time. After 72 h of treatment, the cell wall areas of *Fagus crenata* in both earlywood and latewood had increased by 4 times, and those of *Quercus mongolica* in earlywood and latewood had increased by 3.5 and 5 times, respectively. However, the swelling behavior of two other species that were tested was different from *Fagus crenata* and *Quercus mongolica*. The cell wall area of *Quercus glauca* in latewood increased gradually with progressing treatment time, but not in the earlywood. The change in cell wall area in *Trochodendron aralioides* levelled off in both earlywood and latewood. After 72 h of treatment, the cell wall areas of *Quercus glauca* in earlywood and latewood had increased by 2 and 3 times, respectively, and those of *Trochodendron aralioides* in earlywood and latewood had increased by 1.5 and 2 times, respectively. Therefore, swelling behavior, including the swelling ratio and time-

http://dx.doi.org/10.5772/62721

dependent change of fibrous cells during [C2mim][Cl] treatment, differed according to the wood species and morphological regions, including earlywood and latewood.

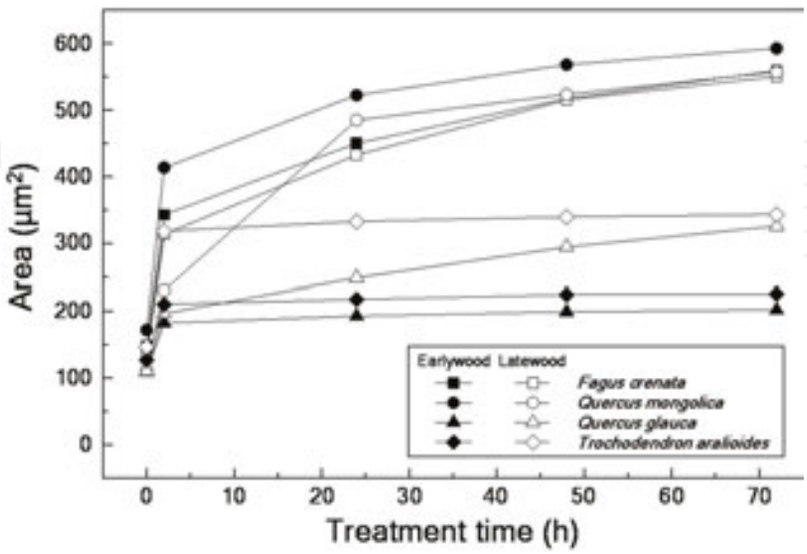

Figure 4. Changes in the cell wall area of fibrous cells in the earlywood and latewood of various wood species during [C2mim][Cl] treatment at 120°C [35, 36].

Figure 5 shows bright-field microscopy and polarized light microscopy images of *Cryptomeria japonica* before and after treatment for 72 h with [EtPy][Br] at 120°C. The cell walls of both earlywood and latewood were swollen by [EtPy][Br] treatment (**Figure 5c**). Although the cell walls in earlywood were well ordered during [EtPy][Br] treatment, those in latewood were partially dissociated. After 72 h of treatment, tracheids in earlywood and latewood were

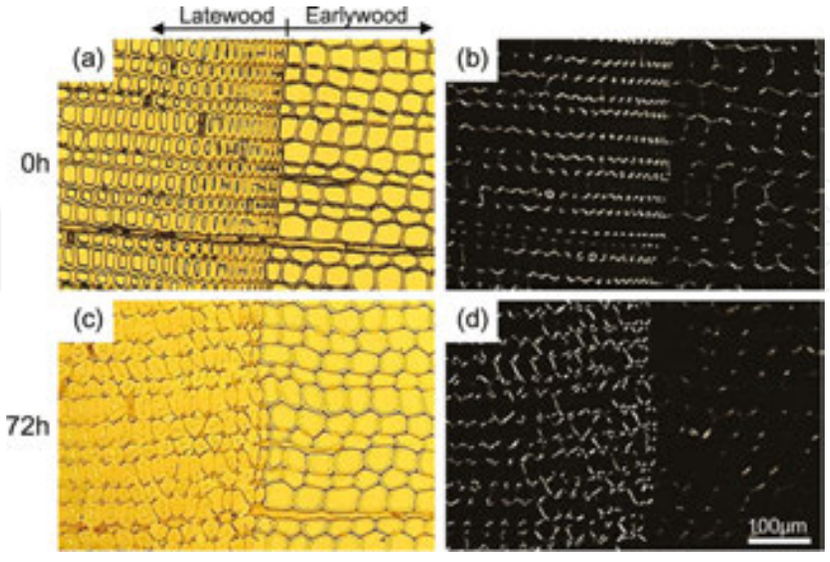

Figure 5. Bright-field microscopy (**a**, **c**) and polarized light microscopy images (**b**, **d**) of transverse sections of *Cryptomeria japonica* before (**a**, **b**) and after treatment with [EtPy][Br] at 120°C for 72 h (**c**, **d**) [37].

swollen by 1.3 and 2 times, respectively. Therefore, the swelling efficiency of [EtPy][Br] is lower than that of [C2mim][Cl]; and morphological changes in wood cell walls differ for the different types of ionic liquids. In the polarized light micrographs, the brightness from the birefringence of cellulose showed no changes during [EtPy][Br] treatment (**Figure 5d**). This result implies that [EtPy][Br] treatment has no marked effect on the crystalline structure of cellulose in the wood cell walls.

2.2. Scanning electron microscopy observations

Ultrastructural changes in wood cell walls due to ionic liquid treatment were observed by SEM [34–38]. **Figure 6** shows SEM images of various tissues of *Cryptomeria japonica* treated with [C2mim][Cl] and [EtPy][Br]. The dissociations and distortions of cell walls were observed in latewood after 72 h of treatment with both [C2mim][Cl] and [EtPy][Br] (**Figure 6e**, **i**). These changes were caused by significant swelling of tracheids in latewood. The magnified view of earlywood (**Figure 6b**, **f**, **j**) and latewood (**Figure 6c**, **g**, **k**), shows the CML (indicated by small arrows) disappeared in both earlywood and latewood after [EtPy][Br] treatment (**Figure 6j**, **k**) but was preserved after [C2mim][Cl] treatment (**Figure 6f**, **g**). These changes may be related to lignin distribution in wood cell walls. CML contains more than 50% lignin, whereas S_2 (indicated by arrowheads) contains about 20% lignin [39]. Our recent research revealed that lignin can be preferentially liquefied by [EtPy][Br] [31], which explains why the CML was liquefied more rapidly than S_2 by [EtPy][Br]. **Figure 6d**, **h**, and **l** shows the changes in bordered pits in earlywood. The torus (indicated by large arrows) in the pits was broken after [C2mim][Cl] treatment, while the warts on the surface of tracheids disappeared after [EtPy][Br]

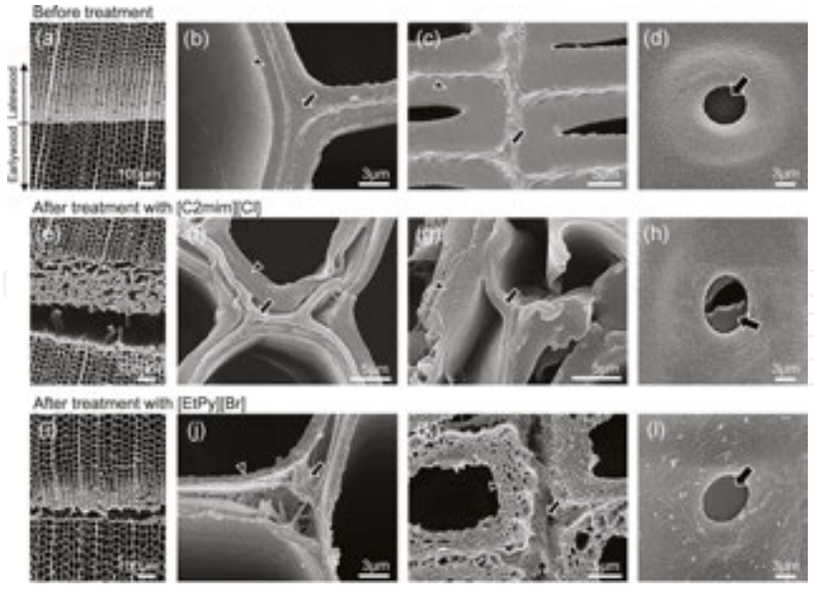

Figure 6. SEM images of various tissues of *Cryptomeria japonica* before (**a**–**d**) and after treatment with [C2mim][Cl] at 120°C for 48 h (**e**–**h**) and with [EtPy][Br] at 120°C for 72 h (**i**–**l**) [37]. (**a**, **e**, **i**) Around the annual ring boundary. (**b**, **f**, **j**), a magnified view of earlywood, (**c**, **g**, **k**) a magnified view of latewood, (**d**, **h**, **l**) bordered pits. The S_2, CML, and torus are indicated by the arrowhead, small arrow and large arrow, respectively.

http://dx.doi.org/10.5772/62721

treatment. Harada and Côté have reported that the torus is mainly composed of cellulose microfibrils [40]. In addition, Jansen et al. stated that warts are mainly composed of lignin and hemicellulose [41]. The differences in the reactivity of [C2mim][Cl] and [EtPy][Br] with these wood tissues derive from differences in their chemical components.

Figure 7 shows SEM images of various tissues of *Fagus crenata* treated with [C2mim][Cl] and [EtPy][Br]. Cracks occurred between the ray parenchyma (indicated by large arrowheads) and peripheral tissues after treatment with both ionic liquids. These changes are presumably due to the bonds between the ray parenchyma and tissues adjacent to it weakening after treatment as well as the difference in the swelling behavior. **Figure 7b**, **f**, and **j** show magnified views of the morphological features of wood fibers treated with [C2mim][Cl] and [EtPy][Br]which are similar to tracheids in latewood of *Cryptomeria japonica* (**Figure 6g**, **k**). Various changes were observed at vessel pits. Intervascular pits (vessel–vessel pits) were occluded after [C2mim][Cl] treatment (**Figure 7g**), while ray-vessel pits were not occluded. Instead, their pit membranes (indicated by large arrows) were broken after the treatment (**Figure 7h**). However, the intervascular pits and ray-vessel pits showed no significant changes after [EtPy][Br] treatment (**Figure 7k**, **l**). These results indicate that morphological changes in the pits differed depending on the types of pits and ionic liquids used.

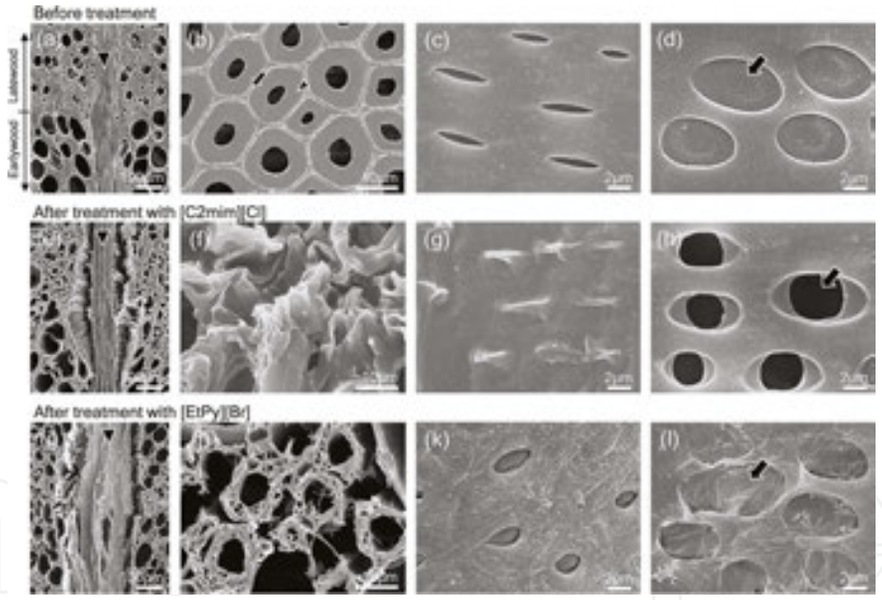

Figure 7. SEM images of various tissues of *Fagus crenata* before (**a**–**d**) and after treatment with [C2mim][Cl] (**e**–**h**) and [EtPy][Br] (**i**–**l**) at 120°C for 72 h [35, 38]. (**a**, **e**, **i**) Around annual ring boundary. (**b**, **f**, **j**) Wood fibers. (**c**, **g**, **k**) Intervascular pits. (**d**, **h**, **l**) Ray-vessel pits. The S_2, CML, ray parenchyma and pit membranes are indicated by the small arrowhead, small arrow, large arrow head and large arrow, respectively.

Figure 8 shows SEM images of transverse sections of two hardwood species treated with [C2mim][Cl]. Although wood fibers (indicated by arrowheads) of both *Fagus crenata* and *Quercus mongolica* showed significant deformation, the axial parenchyma cells (indicated by arrows) maintained their shapes (**Figure 8c**, **d**). These differences in morphological changes between the wood fibers and axial parenchyma cells are mainly attributed to their chemical

composition. Fujii et al. reported that the lignin content of the axial parenchyma cells is higher than that of the wood fibers [42]. In our previous papers, we showed that lignin is much more difficult to react with [C2mim][Cl] than cellulose and hemicellulose [25, 28]. The reactivity of [C2mim][Cl] with the axial parenchyma cells is lower than that with the wood fibers, thus the axial parenchyma cells did not collapse after [C2mim][Cl] treatment.

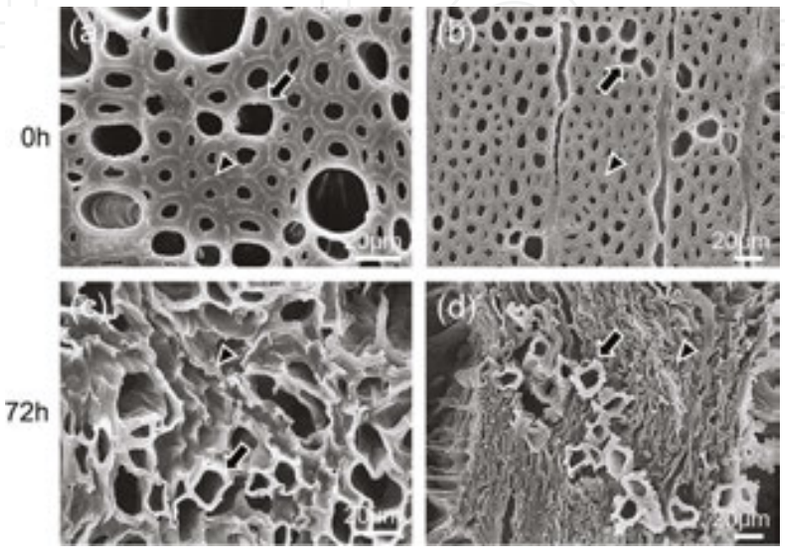

Figure 8. SEM images of transverse sections of *Fagus crenata* (**a**, **c**) and *Quercus mongolica* (**b**, **d**) before and after treatment with [C2mim][Cl] at 120°C for 72 h [35, 36]. Wood fibers and axial parenchyma cells are indicated by arrow heads and arrows, respectively.

2.3. Confocal Raman microscopy analysis

Raman spectra can reveal much information about functional groups, hydrogen and chemical bonds, and the surrounding environment. Raman spectroscopy is used to identify the chemical structure of a substance. Confocal Raman microscopy couples Raman spectroscopy with a confocal microscope to perform detailed analysis quickly. In recent years, confocal Raman microscopy has received attention as a new method of spectroscopic analysis for plant cell walls because of its characteristic advantages. It is non-destructive, has a high spatial resolution (approximately 0.3–2 μm), is not hindered by the presence of water [43, 44], and little-to-no sample pre-treatment is required. Several research groups have studied the chemical composition of native wood cell walls using this method [45–51]. In addition, it has been reported that confocal Raman microscopy is an effective tool to investigate topochemical changes in wood after pre-treatment for biorefinery [52–54].

We applied confocal Raman microscopy to determine the changes in chemical components and their distribution in wood at the cellular level during [C2mim][Cl] and [EtPy][Br] treatment [37, 38, 55, 56]. **Figure 9** shows Raman spectra obtained from S_2 of the wood fibers of *Fagus crenata* treated with [C2mim][Cl] and [EtPy][Br]. The characteristic Raman bands of lignin were observed at 370, 1331, 1459, 1600, 1657, 2848, and 2943 cm^{-1}, whereas those of the polysaccharides (cellulose and hemicellulose) were observed at 380, 436, 520, 1093, 1118, 1152,

http://dx.doi.org/10.5772/62721

1378, and 2895 cm^{-1}. These band assignments were based on previous studies [57–61]. Although all the band intensities of the polysaccharides sharply decreased during [C2mim][Cl] treatment, most band intensities of lignin barely changed, except for some bands (**Figure 9a**). For instance, the band intensity at 1657 cm^{-1} was assigned to the ethylenic C=C bond in coniferyl/sinapyl alcohol units and γ—C=O in coniferyl/sinapyl aldehyde units decreased gradually. These results indicate that [C2mim][Cl] prefers to react with polysaccharides in S_2 of wood fibers rather than with lignin, despite the molecular structures of lignin changing partially during [C2mim][Cl] treatment. Regarding time-dependent spectral changes during [EtPy][Br] treatment, most band intensities of polysaccharides showed no significant changes, while those of lignin decreased with prolonged treatment time (**Figure 9b**). These spectral changes indicate that lignin is liquefied more readily than polysaccharides in [EtPy][Br].

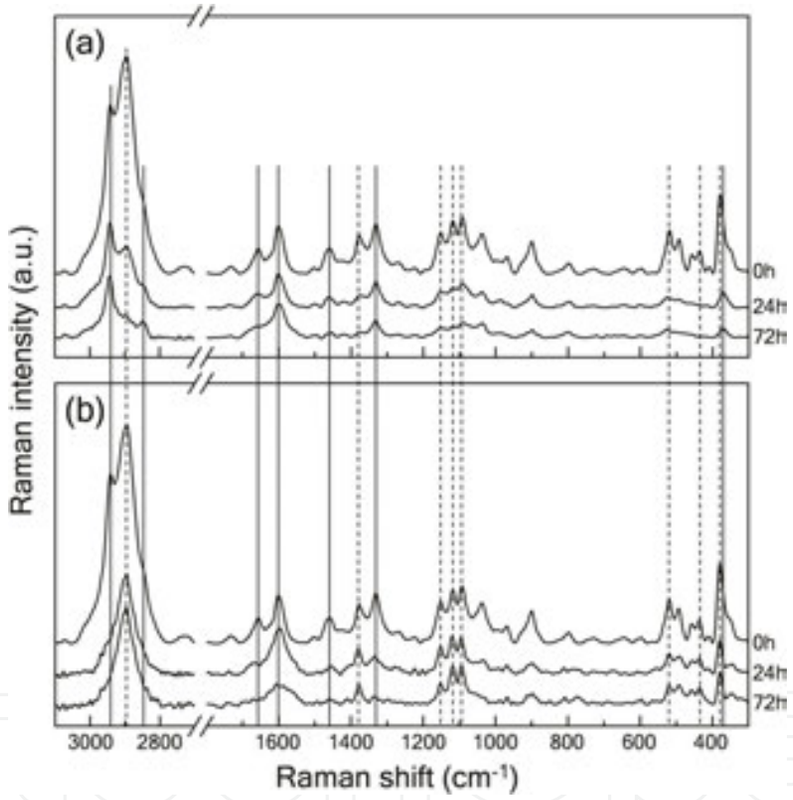

Figure 9. Raman spectra for the S_2 of wood fibers of *Fagus crenata* after treatment with [C2mim][Cl] (**a**) and [EtPy][Br] (**b**) at 120°C for 0 h, 24 h, and 72 h. Lignin and polysaccharides are indicated by solid lines and dashed lines respectively. [38, 56].

To study the changes in the distribution of chemical components in the wood cell walls over a wide range during ionic liquids treatment, Raman mapping analysis was applied on transverse sections. Raman mapping was performed on tracheids and wood fibers because these tissues are the main elements of *Cryptomeria japonica* and *Fagus crenata*, respectively. In the Raman images, bright areas indicate high concentrations of a specific chemical composition, whereas dark areas indicate low concentrations.

Figure 10 shows the results of time-sequential Raman mapping analysis of the distribution of lignin and polysaccharides of tracheids of *Cryptomeria japonica* and wood fibers of *Fagus crenata* during [C2mim][Cl] treatment. Within both wood species, the lignin concentration was higher in CML than in S_2 while the polysaccharide concentrations were lower in CML than in S_2. After treatment, changes in the distribution of chemical compositions were similar for the tracheids of *Cryptomeria japonica* and wood fibers of *Fagus crenata*. Although the lignin concentration in S_2 decreased with increasing [C2mim][Cl]treatment time, the concentration in CML showed no significant change. These results indicate that lignin in CML has a high chemical resistance to [C2mim][Cl]. The differences in the reactivity of [C2mim][Cl] with lignin in each morphological region are attributed to many factors such as molecular structure, concentration, and penetrability of [C2mim][Cl]. Polysaccharide concentrations decreased significantly after 24 h of treatment. After that, most of the Raman signal derived from polysaccharides disappeared. Therefore, in fibrous cells of wood, polysaccharides were more rapidly liquefied by [C2mim][Cl] than lignin.

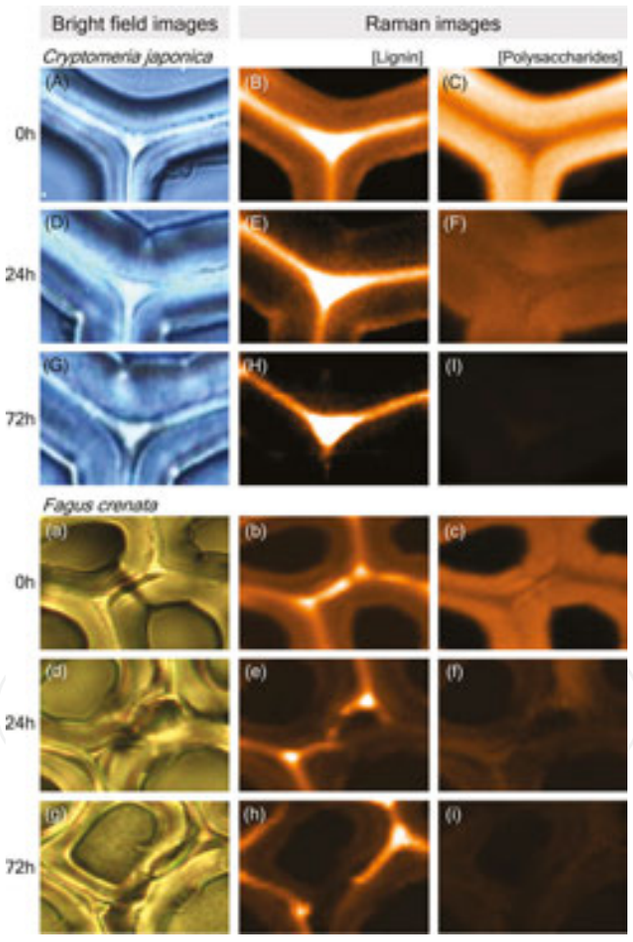

Figure 10. Raman mapping of transverse sections of tracheids of *Cryptomeria japonica* (**A–I**) and wood fibers of *Fagus crenata* (**a–i**) before and after treatment with [C2mim][Cl] at 120°C for 0 h, 24 h, and 72 h [55, 56]. The left panel shows bright field images of the measured position, the middle panel shows the distribution of lignin, the right panel shows the distribution of polysaccharides. Bright regions indicate high concentrations of specific chemical compositions, dark regions indicate low concentrations.

http://dx.doi.org/10.5772/62721

Raman mapping analysis was also performed on the wood samples treated with [EtPy][Br] (**Figure 11**). Although the lignin concentration in S_2 and in CML decreased with prolonged treatment time, the lignin in CML was preserved at relatively high concentration after 72 h of treatment in both tracheids of *Cryptomeria japonica* and wood fibers of *Fagus crenata*. Polysaccharide concentrations in both species decreased after 24 h of treatment. However, after 72 h of treatment, the polysaccharide concentrations in the tracheids of *Cryptomeria japonica* showed no significant changes, while those in the wood fibers of *Fagus crenata* continued to decrease gradually. These results imply that the reactivity of [EtPy][Br] with lignin is higher than with the polysaccharides in S_2 of fibrous cells. In addition, the liquefaction behavior of polysaccharides in fibrous cells during [EtPy][Br] treatment is different for different wood species.

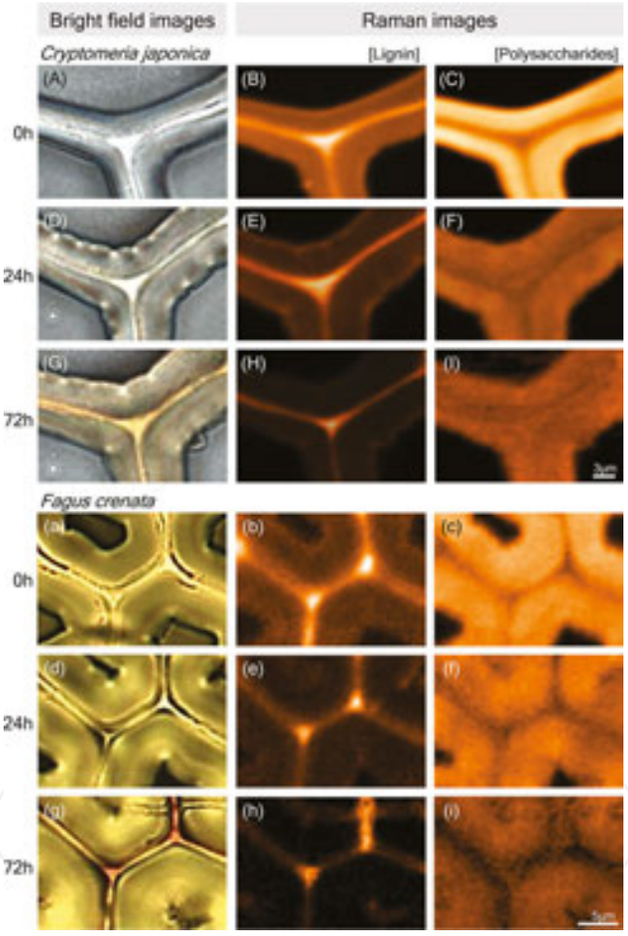

Figure 11. Raman mapping on transverse sections of tracheids of *Cryptomeria japonica* (**A–I**) and wood fibers of *Fagus crenata* (**a–i**) before and after treatment with [EtPy][Br] at 120°C for 0 h, 24 h, and 72 h [37, 38]. The left panel shows bright field images of the measured position, the middle panel shows the distribution of lignin, the right panel shows the distribution of polysaccharides. Bright regions indicate high concentrations of specific chemical compositions, dark regions indicate low concentrations.

To gain insight into the reactivity of [C2mim][Cl] with various morphological regions, Raman spectra were acquired for the S_2 of wood fibers, the cell corner of wood fibers, vessels, and axial parenchyma cells of *Fagus crenata* (**Figure 12**). During [C2mim][Cl] treatment, all the polysac-

charide band intensities of S_2 of wood fibers and vessels decreased markedly, whereas those of the axial parenchyma cells decreased slightly. In addition, the intensity of the lignin band at 1657 cm^{-1} decreased significantly for all the measured regions except for the sample of axial parenchyma cells. Overall, the Raman spectra for axial parenchyma cells were not changed by [C2mim][Cl] treatment compared with those for the other morphological regions. This result indicates that both the polysaccharides and lignin of axial parenchyma cells are difficult to react with [C2mim][Cl]. The tendency of the spectral changes agrees with the morphological changes observed by SEM (**Figure 8**).

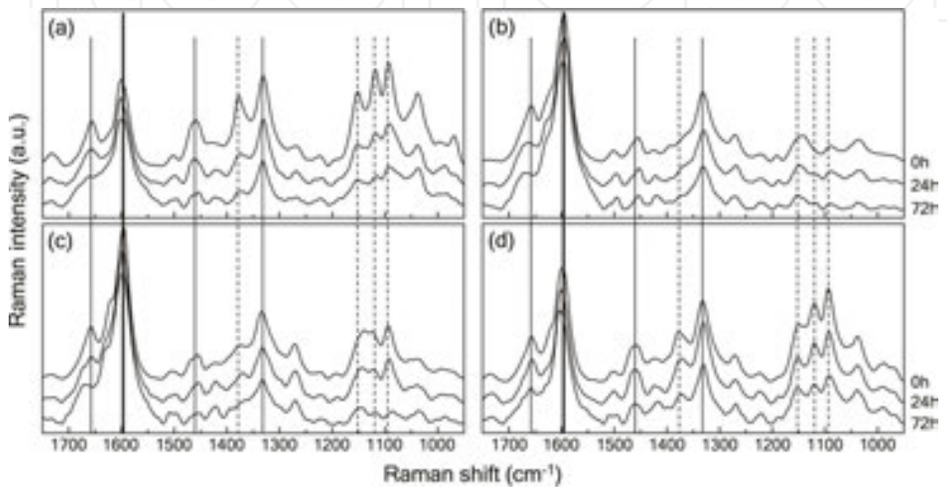

Figure 12. Raman spectra focusing in the spectral region of 950–1750 cm^{-1} for S_2 of wood fibers (**a**), cell corner of wood fibers (**b**), vessels (**c**), and axial parenchyma cells (**d**) of *Fagus crenata* before and after treatment with [C2mim][Cl] at 120°C for 0 h, 24 h, and 72 h; [56]. Lignin and polysaccharides are indicated by solid lines and dashed lines respectively. The spectra were normalized based on the band of an aromatic ring vibration around 1600 cm^{-1} (thick lines), which has superior chemical stability under [C2mim][Cl] treatment conditions, as an internal reference to visualize the spectral differences after treatment with [C2mim][Cl] clearly.

3. Conclusions

Using various microscopy techniques, the morphological and topochemical features of wood cell walls treated with ionic liquids were studied. During the processing of wood liquefaction in ionic liquids, the ultrastructure and chemical compositions of wood showed inhomogeneous changes at the cellular level. The interaction of ionic liquid with wood cell walls was quite different depending on the types of ionic liquids, wood species, tissues, and cell wall layers. These findings will serve to cultivate a better understanding of the liquefaction mechanism of woody biomass in ionic liquids and accelerate development of ionic liquid treatment for wood-based biorefinery.

For research in wood chemistry and anatomy, many microscopy techniques have been applied to investigate the characteristics of the cell walls. However, it is hardly possible to examine the chemical compositions and their distribution with nanoscale spatial resolution while at the

same time observing the ultrastructure such as ultrathin layers. The development of sensitive analytical methods in the wood cell walls for chemical information with much higher spatial resolution will open a new field of wood science and technology.

Acknowledgements

This work was partly supported by the "Science and Technology Research Promotion Program for Agriculture, Forestry, Fisheries and Food Industry" (No. 26052A) from the Ministry of Agriculture, Forestry and Fisheries of Japan, a Grant-in-Aid for Scientific Research (C) (No. 25450246) from the Japan Society for the Promotion of Science (JSPS), and a Grant-in-Aid for JSPS Fellows (No. 15J05592).

Author details

Toru Kanbayashi[1,2] and Hisashi Miyafuji[2*]

*Address all correspondence to: miyafuji@kpu.ac.jp

1 Department of Wood Improvement, Forestry and Forest Products Research Institute, Ibaraki, Japan

2 Graduate School of Life and Environmental Sciences, Kyoto Prefectural University, Kyoto, Japan

References

[1] Zhu JY, Pan X, Zalesny Jr. RS. Pretreatment of woody biomass for biofuel production: energy efficiency, technologies, and recalcitrance. Applied Microbiology and Biotechnology. 2010;87(3):847–857. DOI: 10.1007/s00253-010-2654-8

[2] Pettersen RC. The Chemical Composition of Wood. In: Rowell RM, editor. The Chemistry of Solid Wood, Advances in Chemistry Series, Vol. 207. Washington, DC: American Chemical Society; 1984. p. 57–126.

[3] Taherzadeh MJ, Karimi K. Acid-based hydrolysis processes for ethanol from lignocellulosic materials: a review. BioResources. 2007;2(3):472–499.

[4] Taherzadeh MJ, Eklund R, Gustafsson L, Niklasson C, Liden G. Characterization and fermentation of dilute-acid hydrolyzates from wood. Industrial & Engineering Chemistry Research. 1997;36(11):4659–4665. DOI: 10.1021/ie9700831

[5] Parisi F. Advances in Lignocellulosics Hydrolysis and in the Utilization of the Hydrolyzates. In: Fiechter A, editor. Advances in Biochemical Engineering/Biotechnology, Vol. 38. Berlin: Springer-Verlag; 1989. p. 53–87. DOI: 10.1007/BFb0007859

[6] Chang VS, Holtzapple MT. Fundamental factors affecting biomass enzymatic reactivity. Applied Biochemistry and Biotechnology. 2000;84–86:5–37. DOI: 10.1007/978-1-4612-1392-5_1

[7] Zhao Y, Wang Y, Zhu JY, Ragauskas A, Deng Y. Enhanced enzymatic hydrolysis of spruce by alkaline pretreatment at low temperature. Biotechnology and Bioengineering. 2008;99(6):1320–1328. DOI: 10.1002/bit.21712

[8] Piskorz J, Radlein D, Scott DS, Czernik S. Liquid Products from the Fast Pyrolysis of Wood and Cellulose. In: Bridgwater AV, Kuester JL, editors. Research in Thermochemical Biomass Conversion. London: Elsevier Applied Science; 1988. p. 557–571. DOI: 10.1007/978-94-009-2737-7_43

[9] Kwon GJ, Kuga S, Hori K, Yatagai M, Ando K, Hattori N. Saccharification of cellulose by dry pyrolysis. Journal of Wood Science. 2006;52(5):461–465. DOI: 10.1007/s10086-005-0784-x

[10] Hosoya T, Kawamoto H, Saka S. Influence of inorganic matter on wood pyrolysis at gasification temperature. Journal of Wood Science. 2007;53(4):351–357. DOI: 10.1007/s10086-006-0854-8

[11] Oasmaa A, Solantausta Y, Arpiainen V, Kuoppala E, Sipilä K. Fast pyrolysis bio-oils from wood and agricultural residues. Energy & Fuels. 2010;24(2):1380–1388. DOI: 10.1021/ef901107f

[12] Yamazaki J, Minami E, Saka S. Liquefaction of beech wood in various supercritical alcohols. Journal of Wood Science. 2006;52(6):527–532. DOI: 10.1007/s10086-005-0798-4

[13] Xu C, Etcheverry T. Hydro-liquefaction of woody biomass in sub- and super-critical ethanol with iron-based catalysts. Fuel. 2008;87(3):335–345. DOI: 10.1016/j.fuel.2007.05.013

[14] Sheldon R. Catalytic reactions in ionic liquids. Chemical Communications. 2001;23:2399–2407. DOI: 10.1039/B107270F

[15] Seddon KR. Ionic liquids for clean technology. Journal of Chemical Technology and Biotechnology. 1997;68(4):351–356. DOI: 10.1002/(SICI)1097-4660(199704)68:4<351::AID-JCTB613>3.0.CO;2-4

[16] Rogers RD, Seddon KR. Ionic liquids – Solvents of the future? Science. 2003;302(5646):792–793. DOI: 10.1126/science.1090313

[17] Freemantle M. Designer solvents – Ionic liquids may boost clean technology development. Chemical & Engineering News. 1998;76:32–37.

[18] Swatloski RP, Spear SK, Holbrey JD, Rogers RD. Dissolution of cellulose with ionic liquids. Journal of the American Chemical Society. 2002;124(18):4974–4975. DOI: 10.1021/ja025790m

[19] Zhang H, Wu J, Zhang J, He J. 1-Allyl-3-methylimidazolium chloride room temperature ionic liquid: a new and powerful nonderivatizing solvent for cellulose. Macromolecules. 2005;38(20):8272–8277. DOI: 10.1021/ma0505676

[20] Fukaya Y, Hayashi K, Wada M, Ohno H. Cellulose dissolution with polar ionic liquids under mild conditions: required factors for anions. Green Chemistry. 2008;10:44–46. DOI: 10.1039/B713289A

[21] Pu Y, Jiang N, Ragauskas AJ. Ionic liquid as a green solvent for lignin. Journal of Wood Chemistry and Technology. 2007;27(1):23–33. DOI: 10.1080/02773810701282330

[22] Honglu X, Tiejun S. Wood liquefaction by ionic liquids. Holzforschung. 2006;60(5):509–512. DOI: 10.1515/HF.2006.084

[23] Fort DA, Remsing RC, Swatloski RP, Moyna P, Moyna G, Rogers RD. Can ionic liquids dissolve wood? Processing and analysis of lignocellulosic materials with 1-*n*-butyl-3-methylimidazolium chloride. Green Chemistry. 2007;9(1):63–69. DOI: 10.1039/B607614A

[24] Kilpeläinen I, Xie H, King A, Granstrom M, Heikkinen S, Argyropoulos DS. Dissolution of wood in ionic liquids. Journal of Agricultural and Food Chemistry. 2007;55(22):9142–9148. DOI: 10.1021/jf071692e

[25] Miyafuji H, Miyata K, Saka S, Ueda F, Mori M. Reaction behavior of wood in an ionic liquid, 1-ethyl-3-methylimidazolium chloride. Journal of Wood Science. 2009;55(3):215–219. DOI: 10.1007/s10086-009-1020-x

[26] Abe M, Yamada T, Ohno H. Dissolution of wet wood biomass without heating. RSC Advances. 2014;4(33):17136–17140. DOI: 10.1039/C4RA01038H

[27] Sun N, Rahman M, Qin Y, Maxim ML, Rodriguez H, Rogers RD. Complete dissolution and partial delignification of wood in the ionic liquid 1-ethyl-3-methylimidazolium acetate. Green Chemistry. 2009;11(5):646–655. DOI: 10.1039/B822702K

[28] Nakamura A, Miyafuji H, Saka S. Liquefaction behavior of Western red cedar and Japanese beech in the ionic liquid 1-ethyl-3-methylimidazolium chloride. Holzforschung. 2010;64(3):289–294. DOI: 10.1515/hf.2010.042

[29] Nakamura A, Miyafuji H, Saka S. Influence of reaction atmosphere on the liquefaction and depolymerization of wood in an ionic liquid, 1-ethyl-3-methylimidazolium chloride. Journal of Wood Science. 2010;56(3):256–261. DOI: 10.1007/s10086-009-1081-x

[30] Brandt A, Hallett JP, Leak DJ, Murphy RJ, Welton T. The effect of the ionic liquid anion in the pretreatment of pine wood chips. Green Chemistry. 2010;12:672–679. DOI: 10.1039/B918787A

[31] Yokoo T, Miyafuji H. Reaction behavior of wood in an ionic liquid, 1-ethylpyridinium bromide. Journal of Wood Science. 2014;60(5):339-345. DOI: 10.1007/s10086-014-1409-z

[32] Saka S. Chemical Composition and Distribution. In: Hon DNS, Shiraishi N, editors. Wood and Cellulosic Chemistry. New York: Marcel Dekker; 1991. p. 59–88.

[33] Miyafuji H, Suzuki N. Observation by light microscope of sugi (*Cryptomeria japonica*) treated with the ionic liquid 1-ethyl-3-methylimidazolium chloride. Journal of Wood Science. 2011;57:459–461. DOI: 10.1007/s10086-011-1190-1

[34] Miyafuji H, Suzuki N. Morphological changes in sugi (*Cryptomeria japonica*) wood after treatment with the ionic liquid, 1-ethyl-3-methylimidazolium chloride. Journal of Wood Science. 2012;58(3):222–230. DOI: 10.1007/s10086-011-1245-3

[35] Kanbayashi T, Miyafuji H. Morphological changes of Japanese beech treated with the ionic liquid, 1-ethyl-3-methylimidazolium chloride. Journal of Wood Science. 2013;59(5):410–418. DOI: 10.1007/s10086-013-1343-5

[36] Kanbayashi T, Miyafuji H. Comparative study of morphological changes in hardwoods treated with the ionic liquid, 1-ethyl-3-methylimidazolium chloride. Journal of Wood Science. 2014;60(2):152–159. DOI: 10.1007/s10086-014-1389-z

[37] Kanbayashi T, Miyafuji H. Topochemical and morphological characterization of wood cell wall treated with the ionic liquid, 1-ethylpyridinium bromide. Planta. 2015;242(3): 509–518. DOI: 10.1007/s00425-014-2235-7

[38] Kanbayashi T, Miyafuji H. Anatomical and topochemical aspects of Japanese beech (*Fagus crenata*) cell walls after treatment with the ionic liquid, 1-ethylpyridinium bromide. Microscopy and Microanalysis. 2015;21(6):1562–1572. DOI: 10.1017/S1431927615015275

[39] Donaldson LA, Lignification and lignin topochemistry – an ultrastructural view. Phytochemistry. 2001;57(6):859–873. DOI: 10.1016/S0031-9422(01)00049-8

[40] Harada H, Côté WA. Structure of Wood. In: Higuchi T, editor. Biosynthesis and Biodegradation of Wood Components. Orlando: Academic Press; 1985. p. 1–42.

[41] Jansen S, Smets E, Baas P. Vestures in woody plants: a review. IAWA Journal. 1998;19(4):347–382. DOI: 10.1163/22941932-90000658

[42] Fujii T, Shimizu K, Yamaguchi A. Enzymatic saccharification on ultrathin sections and ultraviolet spectra of Japanese hardwoods and softwoods. Mokuzai Gakkaishi. 1987;33(5):400–407.

[43] Fackler K, Thygesen LG. Microspectroscopy as applied to the study of wood molecular structure. Wood Science and Technology. 2013;47(1):203–222. DOI: 10.1007/s00226-012-0516-5

[44] Lupoi JS, Singh S, Simmons BA, Henry RJ. Assessment of lignocellulosic biomass using analytical spectroscopy: an evolution to high-throughput techniques. BioEnergy Research. 2014;7(1):1–23. DOI: 10.1007/s12155-013-9352-1

[45] Agarwal UP. Raman imaging to investigate ultrastructure and composition of plant cell walls: distribution of lignin and cellulose in black spruce wood (*Picea mariana*). Planta. 2006;224:1141–1153. DOI: 10.1007/s00425-006-0295-z

[46] Gierlinger N, Schwanninger M. Chemical imaging of poplar wood cell walls by confocal Raman microscopy. Plant Physiology. 2006;140(4):1246–1254. DOI: 10.1104/pp.105.066993

[47] Röder T, Koch G, Sixta H. Application of confocal Raman spectroscopy for the topochemical distribution of lignin and cellulose in plant cell walls of beech wood (*Fagus sylvatica* L.) compared to UV microspectrophotometry. Holzforschung. 2004;58(5):480–482. DOI: 10.1515/HF.2004.072

[48] Schmidt M, Schwartzberg AM, Perera PN, Weber-Bargioni A, Carroll A, Sarkar P, Bosneaga E, Urban JJ, Song J, Balakshin MY, Capanema EA, Auer M, Adams PD, Chiang VL, James Schuck P. Label-free in situ imaging of lignification in the cell wall of low lignin transgenic *Populus trichocarpa*. Planta. 2009;230(3):589–597. DOI: 10.1007/s00425-009-0963-x

[49] Hänninen T, Kontturi E, Vuorinen T. Distribution of lignin and its coniferyl alcohol and coniferyl aldehyde groups in *Picea abies* and *Pinus sylvestris* as observed by Raman imaging. Phytochemistry. 2011;72(14–15):1889–1895. DOI: 10.1016/j.phytochem.2011.05.005

[50] Sun L, Simmons BA, Singh S. Understanding tissue specific compositions of bioenergy feedstocks through hyperspectral Raman imaging. Biotechnology and Bioengineering. 2011;108(2):286–295. DOI: 10.1002/bit.22931

[51] Zhang Z, Ma J, Ji Z, Xu F. Comparison of anatomy and composition distribution between normal and compression wood of *Pinus bungeana* Zucc. revealed by microscopic imaging techniques. Microscopy and Microanalysis. 2012;18(6):1459–1466. DOI: 10.1017/S1431927612013451

[52] Ma J, Zhang X, Zhou X, Xu F. Revealing the changes in topochemical characteristics of poplar cell wall during hydrothermal pretreatment. BioEnergy Research. 2014;7(4):1358–1368. DOI: 10.1007/s12155-014-9472-2

[53] Ji Z, Ma J, Xu F. Multi-scale visualization of dynamic changes in poplar cell walls during alkali pretreatment. Microscopy and Microanalysis. 2014;20(2):566–576. DOI: 10.1017/S1431927614000063

[54] Zhou X, Ma J, Ji Z, Zhang X, Ramaswamy S, Xu F. Dilute acid pretreatment differentially affects the compositional and architectural features of *Pinus bungeana* Zucc. compression and opposite wood tracheid walls. Industrial Crops and Products. 2014;62:196–203. DOI: 10.1016/j.indcrop.2014.08.035

[55] Kanbayashi T, Miyafuji H. Raman microscopic analysis of wood after treatment with the ionic liquid, 1-ethyl-3-methylimidazolium chloride. Holzforschung. 2015;69(3): 273–279. DOI: 10.1515/hf-2014-0060

[56] Kanbayashi T, Miyafuji H. Raman microscopic study of Japanese beech (*Fagus crenata*) as treated with the ionic liquid, 1-ethyl-3-methylimidazolium chloride. Journal of Wood Chemistry and Technology. 2016;36(3):224–234. DOI: 10.1080/02773813.2015.1112404

[57] Wiley JH, Atalla RH. Band assignments in the Raman spectra of celluloses. Carbohydrate Research. 1987;160:113–129. DOI: 10.1016/0008-6215(87)80306-3

[58] Agarwal UP, Ralph SA. FT-Raman spectroscopy of wood: Identifying contributions of lignin and carbohydrate polymers in the spectrum of black spruce (*Picea mariana*). Applied Spectroscopy. 1997;51(11):1648–1655. DOI: 10.1366/0003702971939316

[59] Edwards HGM, Farwell DW, Webster D. FT Raman microscopy of untreated natural plant fibres. Spectrochimica Acta Part A: Molecular and Biomolecular Spectroscopy. 1997;53(13):2383–2392. DOI: 10.1016/S1386-1425(97)00178-9

[60] Agarwal UP. An Overview of Raman Spectroscopy as Applied to Lignocellulosic Materials. In: Argyropoulos DS, editor. Advances in Lignocellulosics Characterization. Atlanta: TAPPI Press; 1999. p. 201–225.

[61] Agarwal UP, McSweeny JD, Ralph SA. FT-Raman investigation of milled wood lignins: Softwood, hardwood, and chemically modified black spruce lignins. Journal of Wood Chemistry and Technology. 2011;31(4):324–344. DOI: 10.1080/02773813.2011.562338

IntechOpen